Domain Decomposition Technique for Predicting Cross-Ventilation of Buildings

T. Nonaka and T. Kurabuchi
Tokyo University of Science
M. Ohba
Tokyo Polytechnic University
T. Endo
Kanto Gakuin University

ABSTRACT

Domain decomposition technique is a method for CFD simulation, which can handle internal airflow of cross-ventilation of dwellings separately from external domain. Boundary conditions for internal airflow simulation were picked from calculated result of external domain. Cross-ventilation flow rate was predicted by applying Local dynamic similarity model for large openings. Simulated results were compared with experimental results and good correspondence was observed with respect to cross-ventilation flow rate. Furthermore, general flow pattern predicted by domain decomposition technique was corresponded well to full flow field simulation.

1. INTRODUCTION

Cross-ventilation during hot humid periods is useful for improving indoor thermal environments, and is an important approach for reducing energy used in air-conditioning. Numerous predictions of airflow environments using Computational Fluid Dynamics (CFD) have been done in recent years, and there are more than a few examples of applications in building ventilation planning. For urban housing, where a building is surrounded on all sides and conditions make it difficult to use cross-ventilation, the design must be optimized using numerous case studies of factors such as the arrangement of openings. Computers have made remarkable progress in recent years, but studies of cross-ventilation must be done under various wind direction conditions. Therefore, it is difficult in practice to conduct airflow simulations for many arrangements of openings, over a wide range including the surroundings of the subject building (hereafter this will be called the "full flow field"). Thus, this report proposes a "domain decomposition technique" where calculation of the full flow field and calculation of indoor airflow are done separately, in order to efficiently calculate and predict changes in the cross-ventilation flow rate and indoor airflow structure due to changes in the position of openings. The first part of this report describes the domain decomposition technique. Then the validity of the technique is verified by comparing with the calculation for the full flow field (which also recreates the indoor situation during cross-ventilation) and wind tunnel experiments.

2. OUTLINE OF DOMAIN DECOMPOSITION TECHNIQUE

Figure 1 shows the procedure of indoor airflow analysis using the domain decomposition technique. First, the airflow structure of the full flow field is determined by simulating the airflow around and including the subject building, with all of its openings closed. Boundary conditions are picked up from the obtained airflow conditions acting on the subject building, and then airflow calculation is conducted taking only the inside of the building as the object of analysis. A subroutine for setting boundary conditions is incorporated into the indoor airflow calculations so that the inflow/outflow rate of each opening at this time

is a value based on the discharge coefficient Cd for the opening, estimated using the local dynamic similarity model. Since calculation of the full flow field and calculations of the indoor flow field are separated in this way, there is no need to redo the calculation of the full flow field when the positions of openings are changed.

2.1 *Determination of discharge coefficient based on the Local Dynamic Similarity Model*

Equation (1) based on the discharge coefficient is in general use, and is used here to determine the cross-ventilation flow rate in the building.

$$Q = C_d A\sqrt{\frac{2}{\rho}(P_w - P_R)} \quad \text{(inflow condition)}$$

$$= C_d A\sqrt{\frac{2}{\rho}(P_R - P_w)} \quad \text{(outflow condition)} \quad (1)$$

Here, Q is the cross-ventilation flow rate (m^3/s), C_d is the discharge coefficient, A is the opening area (m^2), ρ is the density (kg/m^3), P_w is the wind pressure at the opening (Pa), and P_R is the internal pressure (Pa).

However, the discharge coefficient varies due to the effects on the opening, of the airflow component tangential to the opening. Therefore, it is known that the prediction error of the cross-ventilation flow rate will increase in some cases if it is treated as a constant.

To address this problem, we have found that the dynamic structure of airflow near the opening achieves similarity under the condition of matching by the non-dimensional internal pressure P_R^*, defined in Equation (2) as the ratio of the ventilation drive P_R-P_W to the tangential dynamic pressure at the opening position P_t.

$$P_R^* = \frac{P_R - P_w}{P_t} \quad (2)$$

Therefore, the discharge coefficient C_d is uniquely determined by P_R^*, and this relationship is called the local dynamic similarity model (LDSM). By clarifying the relationship of C_d and P_R^* using the local dynamic similarity model, it has been confirmed that, for openings with a simple shape close to a square, the relationship can be expressed approximately using Equation (3), as shown in Figure 2.

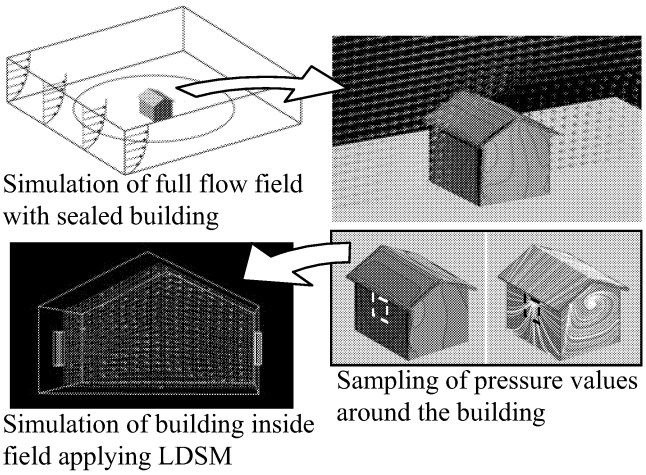

Figure 1. Outline of domain decomposition technique

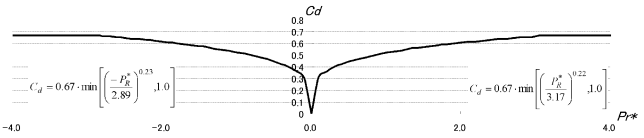

Figure 2. Relation of dimensionless room pressure PR* and discharge coefficient Cd

$$C_d = C_{ds} \cdot min\left[\left(\frac{-P_R^*}{P_{RS1}^*}\right)^{n1}, 1.0\right]$$

(inflow condition: $P_R^* < 0$)

$$= C_{ds} \cdot min\left[\left(\frac{P_R^*}{P_{RS2}^*}\right)^{n2}, 1.0\right]$$

(outflow condition: $P_R^* > 0$) (3)

Here, C_{ds} is the upper limit of the discharge coefficient (= 0.67), P_{RS1}^* and P_{RS2}^* are the absolute values of P_R^* when the discharge coefficient reaches C_{ds} at the inflow opening or outflow opening, n_1 and n_2 are exponents of the change in discharge coefficient at the discharge opening and outflow opening, and min (A, B) is the minimum of A and B.

With LDSM, it is assumed that the tangential dynamic pressure at the opening P_t is not affected by the cross-ventilation flow rate, and thus when P_R^* is determined, the inflow angle of airflow from the opening to the inside is also determined.

2.2 *Simulation procedure for building inside domain*

In the developed method, the boundary conditions set for openings are incorporated into the CFD calculation of indoor airflow as a subroutine, and correction of inflow/outflow boundary conditions is performed in an alternating fashion with the iterative calculation. It is assumed that the wind pressure (inflow side P_{w1}, outflow side P_{w2}) and tangential dynamic pressure (inflow side P_{t1}, outflow side P_{t2}) at the opening position are known from the calculation for the full flow field.

Initial values ${}^0C_{d1}$ and ${}^0C_{d2}$ for the discharge coefficients C_{d1} and C_{d2} at the inflow and outflow opening are set to C_{ds}.

$$ {}^0C_{d1} = {}^0C_{d2} = C_{ds} \qquad (4) $$

Next, the resultant value ${}^0(C_dA)$ is found from Equation (5) by letting A_1 and A_2 be the area of the inflow and outflow opening. Then the initial value of the cross-ventilation flow rate ${}^0Q$ is calculated from Equation (6).

$$ \left(\frac{1}{{}^0(C_dA)}\right)^2 = \left(\frac{1}{{}^0C_{d1}A_1}\right)^2 + \left(\frac{1}{{}^0C_{d2}A_2}\right)^2 \qquad (5) $$

$$ {}^0Q = {}^0(C_dA)\sqrt{\frac{2}{\rho}|P_{w1} - P_{w2}|} \qquad (6) $$

Wind velocity in the normal direction at the inflow opening is set using Equation (7) and the calculated cross-ventilation flow rate, and the same is done for the outflow opening.

$$ {}^0u = \frac{{}^0Q}{A_1} \qquad (7) $$

Here, ${}^0u$ is the wind velocity component in the direction normal to the opening.

The wind velocity component in the tangential direction at the inflow opening is set by assuming that the value from the case with no opening is maintained. For the wind velocity component in the tangential direction at the outflow opening, conditions are given with no gradient, assuming that there are no external influences. For the internal pressure P_R, it is fine to assume any appropriate initial value ${}^0P_R$, but here (for example) a value back-calculated from the cross-ventilation flow rate in Equation (6) can be uniformly given.

The iterative calculation of CFD for the indoor side is started based on the above initial conditions. The CFD calculation is stopped when the solution for indoor airflow has stabilized, and the inflow boundary conditions are then corrected according to the following algorithm.

First, a representative value for indoor static pressure is calculated as a volume average, as indicated in Equation (8), and this is taken to be the internal pressure ${}^kP_R$.

$$ {}^kP_R = \frac{\Sigma P_{si}V_i}{\Sigma V_i} \qquad (8) $$

Here, k is the iteration number of the correction algorithm, P_{si} is the static pressure of the control volume comprising the indoor space, and V_i is the volume of each control volume.

The opening discharge coefficients ${}^kC_{d1}$ and ${}^kC_{d2}$ are calculated by substituting the calculated internal pressure into Equation (2), finding the non-dimensional internal pressure at the inflow opening and outflow opening (${}^kP_{R1}{}^*$ and ${}^kP_{R2}{}^*$) using Equation (9), and then substituting the result into Equation (3).

$$ {}^kP^*_{R1} = \frac{{}^kP_R - P_{w1}}{P_{t1}} \quad , \quad {}^kP^*_{R2} = \frac{{}^kP_R - P_{w2}}{P_{t2}} \qquad (9) $$

Next, the inflow and outflow rate are calculated using Equation (10), and the flow rate residual is calculated from Equation (11).

$$ {}^kQ_1 = {}^kC_{d1}A_1\sqrt{\frac{2}{\rho}\left(P_{w1} - {}^kP_R\right)} \quad , $$

$$ {}^kQ_2 = {}^kC_{d2}A_2\sqrt{\frac{2}{\rho}\left(P_{w2} - {}^kP_R\right)} \qquad (10) $$

$$ \Delta Q = {}^kQ_1 - {}^kQ_2 \qquad (11) $$

If ΔQ does not satisfy the convergence criterion, then the internal pressure is corrected according to Equations (12) and (13).

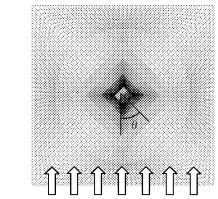

Mesh configuration of full flow field

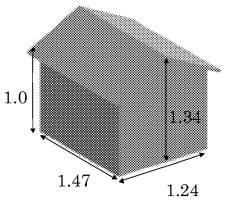

Building geometry

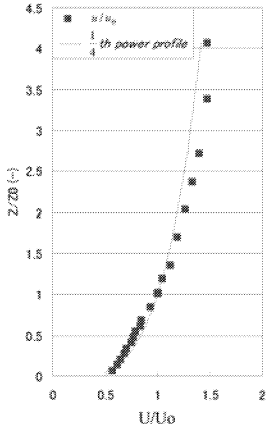

Inflow profile of flow velocity

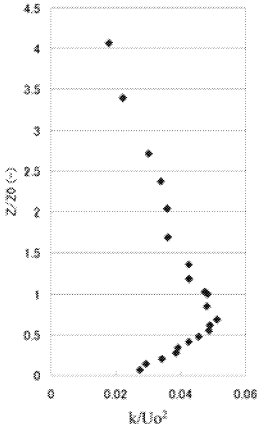

Inflow profile of turbulent kinetic energy

Figure 3. Case study of domain decomposition technique

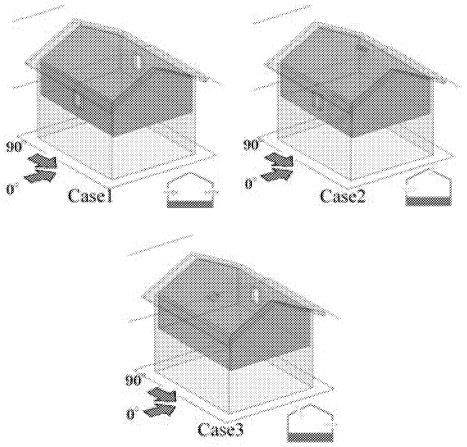

Figure 4. Building inside configuration and opening conditions

$$\Delta P_R = -\frac{\Delta Q}{\frac{\partial \Delta Q}{\partial P_R}} \quad (12)$$

$$^{k+1}P_R = {}^{k}P_R + \alpha \Delta P_R \quad (13)$$

Here, α is the correction relaxation coefficient for internal pressure (α < 1)

The inflow rate and outflow rate are calculated again based on the internal pressure corrected according to the procedure above, and correction of the internal pressure is repeated until the residue satisfies the convergence criterion. Boundary conditions and internal pressure are set based on the flow rate at the time of convergence, and iterative calculation of CFD is resumed.

3. APPLICAION EXAMPLES OF SOLUTION PROCEDURE CALCULATION CONDITIONS

In order to show the validity of the calculation method, the indoor cross-ventilation environment was calculated, assuming, for simplicity, a building with no surrounding obstructions, as shown in Figure 3. The calculation mesh used for airflow around the building was configured by dividing into a cylindrical domain covering the area around the building, and a peripheral domain outside that. An urban area was assumed for the inflow boundary conditions, with the profile set in wind tunnel experiments roughly in accordance with a 1/4 power profile, as shown in Figure 3, and free outflow (parameter gradient 0) was assumed for the outflow boundary conditions. An improved k-e model, with the turbulence time scale of the standard k-ε model constrained using a Durbin limiter, was used to improve the predictive accuracy of the wind pressure coefficient. Three cases (1–3) combining wall surfaces and a skylight for the 2-story part, as shown in Figure 4, were considered for openings in the building. First, airflow around the building was calculated by rotating the cylindrical domain, assuming 3 cases for the wind direction angle (0, 45 and 90°). After that, indoor airflow calculation for the 3 opening cases was performed for each wind direction, so a total of 9 cases were examined. A CFD calculation of the full flow field, with a recreation of the indoor part, was also done, and these were all compared against each other.

3.1 *Comparison of pressure distribution around the building*

Figure 5 shows a comparison of wind tunnel experiment results and CFD results with regard to distribution of the wind pressure coefficient Pw outside of the building for each wind direction angle. As can be seen, overestimation at the building wind top surface and underestimation at the roof ridge, which are characteristic of the k-e model, were improved by using an improved k-e model, and the correspondence is extremely good. Figure 6 shows a comparison of experiment and calculation for the wind pressure coefficient Pw. There is clearly a rough correspondence, and no

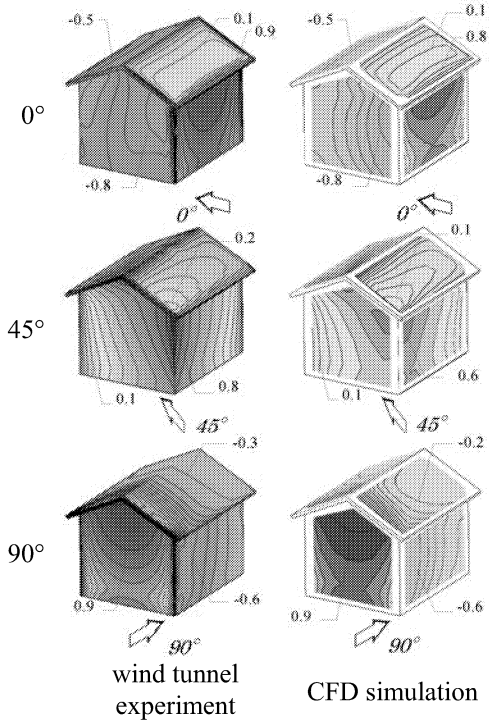

Figure 5. Comparison of observed and predicted of wind pressure coefficient

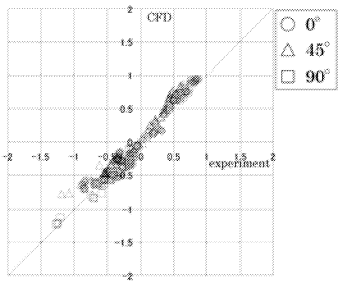

Figure 6. Correspondence of wind pressure coefficient

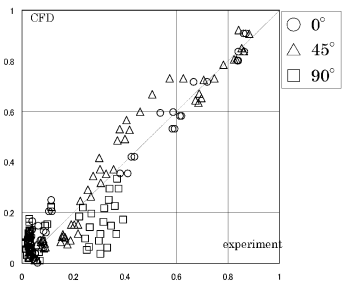

Figure 7. Correspondence of dynamic pressure coefficient tangential to wall

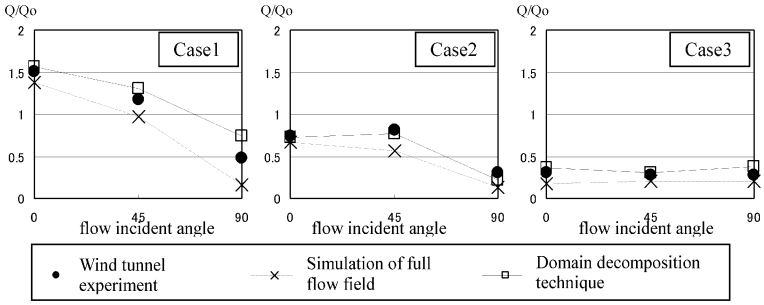

Figure 8. Comparison of observed and predicted cross-ventilation flow rate

dependence on the set wind direction. Figure 7 shows a comparison of CFD with tangential dynamic pressure Pt at the wall surface, measured using an Irwin sensor at a point separated from the wall surface by 1/4 of the opening dimension described below. Compared with the wind pressure coefficient, the variation is quite large, but there is a rough correspondence. This showed that it is possible to accurately predict the pressure distribution at the building surface using CFD.

3.2 *Comparison of cross-ventilation flow rate*

Figure 8 compares the cross-ventilation flow rates—calculated using the domain decomposition technique, with changes in the wind direction, for each opening case—against wind tunnel experiment results and calculation results for the full flow field, including the indoor part. The cross-ventilation flow rate in wind tunnel experiments was measured by dosing tracer gas into the building model interior. The figure shows that, for the domain decomposition technique and all calculation results for the full flow field including the indoor part, changes in the cross-ventilation flow rate are roughly captured in the wind tunnel experiment results, but the cross-ventilation flow rate calculated with the full flow field is somewhat lower than that in experiments. On the other hand, calculation precision is considerably improved with the domain decomposition technique. This is thought to be because there are limits on the accurate reproduction of cross-ventilation airflow involving large acceleration or deceleration of the flow direction, even when the improved k-e model is used. Since the domain decomposition technique only predicts the pressure distribution outside the sealed model, and does not directly address cross-ventilation phenomena, it is likely that the defects of the turbulence model will not manifest themselves.

3.3 *Comparison of flow patterns inside the building*

Figure 9 show a comparison of typical cross-sectional flow patterns, reproduced for each opening case, in calculations using the domain decomposition technique, and calculations using the full flow field, including the indoor part. Since the flow patterns have not been verified with wind tunnel experiments, calculation results for the full flow field are not

necessarily correct. In Case 1, there are wall surface openings for both inflow and outflow, and the inflow angle has a big impact on the indoor airflow pattern. This corresponds well with the airflow pattern in the horizontal cross-section shown in Figure 9. However, diffusion of the incoming airflow is somewhat smaller in the results of the domain decomposition technique. There is a good general correspondence between the results for the domain decomposition technique and the calculation results using the full flow field, but differences are evident in the details. The cause of this is thought to be that the distribution of the incoming airflow within the openings is not taken into account with the domain decomposition technique, but future experimental verification will be necessary.

4. CONCLUTIONS

In this research, a domain decomposition technique was developed, as a technique for efficiently investigating cross-ventilation airflow. With this technique, the airflow around a building and the airflow inside it are examined separately. Wind pressure and tangential dynamic pressure at the building periphery were picked up from the results of analyzing airflow around the building. Then boundary conditions, determined by applying the local dynamic similarity model, were set, and passed to the indoor airflow calculation. The calculation technique was applied to a house with no surrounding buildings, and a comparison was done between wind tunnel experiments and calculation results on the full flow field including the indoor part. This showed that, in terms of airflow around the building, results matching experiments could be obtained for wind pressure and tangential dynamic pressure by using an improved k-e model; that the domain decomposition technique gives better correspondence with experiment than calculation results using the full flow field with regard to the cross-ventilation flow rate; and that, in terms of the indoor flow pattern, there is a rough correspondence between the results of the domain decomposition technique and calculation results using the full flow field including the indoor part. Issues for the future will be verifying the validity of the method

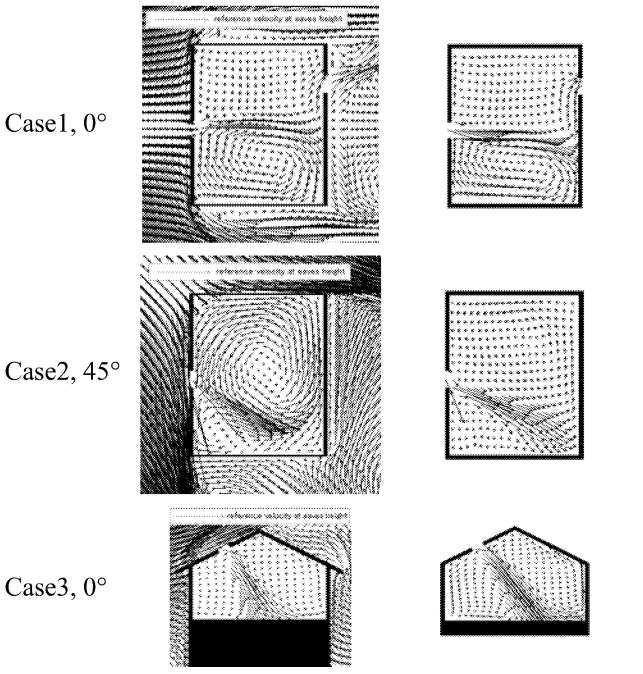

Figure 9. Comparison of cross-ventilation flow pattern inside of the building

when it is applied to conditions where the surrounding area is built up, applying it to other situation such as the condition where there are multiple linked rooms to be ventilated, and verifying the predictive accuracy of indoor flow patterns using wind tunnel experiments.

REFERENCES

Kurabuchi T, Ohba M, Endo T, Akamine Y, and Nakayama F (2004). Local Dynamic Similarity Model of Cross-Ventilation Part 1, Int. J. of Ventilation, vol. 2, No. 4

Ohba M., Goto T., Kurabuchi T., Endo T., and Akamine Y (2006). Experimental study on Predicting Wind- Driven Cross-Ventilation Flow Rates and Discharge Coefficients Based on the Local Dynamic Similarity Model, The Int. J. of Ventilation, Vol. 5, No. 1.

Durbin P.A (1996). On the k-e stagnation point anomaly, Int. J. Heat and Fluid, 17.

Endo T., Kurabuchi T., Ishii M., Komamura K., Maruta E., and Sawachi T. (2005). Study on the Numerical Predictive Accuracy of Wind Pressure Distribution and Air Flow Characteristics – Part1-2, The Int. J. of Ventilation, Vol. 4, No. 3.

Irwin HPAH (1981). A simple omni directional sensor for wind-tunnel studies of pedestrian-level winds, J. of Wind Engineering and Industrial Aerodynamics, 7

Kurabuchi T., Ohba M., Goto T., Akamine Y., Endo T. and Kamata M. (2005). Local Dynamic Similarity Concept as Applied to Evaluation of Discharge Coefficients of Cross-Ventilated Buildings, Part1-3, The Int. J. of Ventilation, Vol.4, No.3.